Critical ages in the life-course of the adult brain: nonlinear subcortical aging

Anders M. Fjell[1,2*], Lars T. Westlye[3], Håkon Grydeland[1], Inge Amlien[1], Thomas Espeseth[3,4,5], Ivar Reinvang[3], Naftali Raz[6], Dominic Holland[7], Anders M Dale[7,8,9], Kristine B. Walhovd[1,2], the Alzheimer Disease Neuroimaging Initiative**

[1] Research Group for Lifespan Changes in Brain and Cognition, Department of Psychology, University of Oslo, Pb 1084, 0317 Oslo, Norway

[2] Department of Physical medicine and rehabilitation, Unit of neuropsychology, Oslo University Hospital, Norway

[3] Department of Psychology, University of Oslo, Pb 1084, 0317 Oslo, Norway

[4] Division for Mental Health and Addiction, Oslo University Hospital, Oslo, Norway

[5] Department of Biological and Medical Psychology, Faculty of Psychology, University of Bergen, Norway

[6] Department of Psychology and Institute of Gerontology, Wayne State University, Detroit, MI, USA

[7] Multimodal Imaging Laboratory, University of California, SD, La Jolla, CA 92093, USA

[8] Department of Radiology, University of California, SD, La Jolla, CA 92093, USA

[9] Department of Neurosciences, University of California, SD, La Jolla, CA 92093, USA

* Address correspondence to: Anders M. Fjell, Dept of Psychology, Pb. 1094 Blindern, 0317 Oslo, Norway, phone: +47 22 84 51 29, fax: +47 22 84 50 01, e-mail: andersmf@psykologi.uio.no

Abstract

Age-related changes in brain structure result from a complex interplay between various neurobiological processes, which may contribute to more complex trajectories than can be described by simple linear or quadratic models. We used a non-parametric smoothing spline approach to delineate cross-sectionally estimated age-trajectories of the volume of 17 neuroanatomical structures in 1100 healthy adults (18-94 years). Accelerated estimated decline in advanced age characterized some structures, e.g. hippocampus, but was not the norm. For most areas, one or two critical ages were identified, characterized by changes in the estimated rate of change. One year follow up data from 142 healthy older adults (60-91 years) confirmed the existence of estimated change from the cross-sectional analyses for all areas except one (caudate). The cross-sectional and the longitudinal analyses agreed well on the rank order of age effects on specific brain structures (Spearman´s ρ = .91). The main conclusions are that most brain structures do not follow a simple path throughout adult life, and that accelerated decline in high age is not the norm of healthy brain aging.

1. Introduction

The volume of most brain structures shrinks with age, but the degree of change is highly heterogeneous across different structures (Allen et al., 2005, Raz and Rodrigue, 2006). Also, age-related changes result from a complex interplay between various neurobiological processes, which is likely to have different impact in different phases of life. This is likely to produce more complex trajectories than what can be described by linear or the usually employed higher order polynomial (quadratic or even cubic) models (Fjell et al., 2010a). The present study was undertaken with the purpose of estimating trajectories across age of 17 brain structures in a large cross-sectional sample (n = 1100). Parts of these data have been previously published (e.g. Fjell et al., 2009c), and we now re-analyze them by applying a statistical approach (the smoothing spline) sensitive to local changes in estimated rate of change (Fjell et al., 2010a). This makes it possible to identify critical ages where life-phases characterized by relative stability are followed by periods where estimated atrophy accelerates, or critical ages where periods of estimated reduction eventually level off. The cross-sectional results were compared with longitudinal atrophy rates from a sample of 142 healthy elderly drawn from the Alzheimer Disease Neuroimaging Initiative (ADNI) (previously presented in (Fjell et al., 2009a)).

Previous literature, including reports based on samples overlapping the present, indicates inverse U-shaped trajectories for hippocampus, cerebral WM, cerebellum WM and the brain stem (Allen et al., 2005, Walhovd et al., 2011, Lupien et al., 2007), while U and J-forms have been reported for caudate and the ventricular system (Sullivan et al., 1995, Good et al., 2001, Walhovd et al., 2011). In contrast, mainly linear trajectories have been reported for

amygdala, thalamus, accumbens and putamen (Gunning-Dixon et al., 1998, Jernigan et al., 2001a, Raz et al., 2003, Sullivan et al., 2004, Allen et al., 2005, Alexander et al., 2006, Nunnemann et al., 2007, Abe et al., 2008, Greenberg et al., 2008, Curiati et al., 2009, Walhovd et al., 2011). Both linear and quadratic reductions have been found for pallidum (Abe et al., 2008, Walhovd et al., 2011). The rational for the present study was to go beyond these general trends, by more accurately delineating the trajectories for the different structures across adult life, and to identify critical ages characterized by changes in estimated rate of atrophy. We included volume for 17 major regions and structures estimated from the whole-brain segmentation approach in FreeSurfer (Fischl et al., 2002). Surface-based cortical thickness results were presented in a previous publication (Fjell et al., in press).

2. Materials and Methods

2.1 Samples

2.1.1 Cross-sectional sample: 1100 healthy adults (424 men/ 676 women), with an age range of 76 years (18-94 years, mean = 48, SD = 20) were included, pooled from five independent studies. Distribution of participants across decades are shown in Table 1. All the healthy samples were screened for diseases and history of neurological conditions and dementia, and none of the participants showed signs of cognitive dysfunction. The details of each of the subsamples are described in Supplementary Table 1, but a brief description is provided here: Sample 1 (Walhovd et al., 2005), n = 69, age 20-88 years (mean 51.3); Sample 2 (Espeseth et al., 2008), n = 208, 19-75 years (mean 46.8); Sample 3 is from the Open Access Series of Imaging Studies(www.oasis-brains.org, Marcus et al., 2007), n = 309, 18-94 years

(44.5); Sample 4 (Raz et al., 2004a), n = 191, 18-81 years (47.3); Sample 5 (Fjell et al., 2010; Westlye et al., 2010), n = 323, 20-85 years (50.8).

[Insert Table 1 about here]

2.1.2 Longitudinal sample: The longitudinal sample consisted of 142 (60-90 years, mean age = 75.6 years, 48% females) participants from the Alzheimer Disease Neuroimaging Initiative (ADNI) database (www.loni.ucla.edu/ADNI), followed for one year. The raw data were obtained from the ADNI database, Principal Investigator Michael W. Weiner, VA Medical Center and University of California – San Francisco. The sample is identical to that included in a previous publication (Fjell et al., 2009a), and is included to allow direct statistical comparisons with the cross-sectional results. ADNI eligibility criteria are described at *http://www.adni-info.org/index.php?option=com_content&task=view&id=9&Itemid=43*.

2.2 MRI processing

All scans were obtained from 1.5T magnets from two different manufacturers (Siemens, Erlangen, Germany; General Electric CO, Milwaukee, WI), and from five different models (Siemens: Avanto, Symphony, Sonata, Vision/ GE: Signa). All participants within each sample were scanned on the same scanner. For details of the sequences, please consult Fjell et al. (Fjell et al., 2009b).

Cross-sectional data were processed and analysed with FreeSurfer 4.01 (http://surfer.nmr.mgh.harvard.edu/)(Fischl et al., 2002). A neuroanatomical label is

automatically assigned to each voxel in an MRI volume based on probabilistic information automatically estimated from a manually labeled training set (Fischl et al., 2002). The training set included both healthy persons in the age range 18-87 yrs and a group of Alzheimer's disease patients in the age range 60-87 yrs, and the classification technique employs a registration procedure that is robust to anatomical variability, including the ventricular enlargement typically associated with aging. The technique has previously been shown to be comparable in accuracy to manual labeling (Fischl et al., 2002; Fischl et al., 2004). An atlas-based normalization procedure was used, shown to increase the robustness and accuracy of the segmentations across scanner platforms (Han and Fischl, 2007). For samples 1, 2, 3 and 5, 2-4 MPRAGEs were averaged before pre-processing to increase signal-to-noise (SNR) and contrast-to-noise ratio (CNR). The following structures/ areas were included in the analyses: total brain volume (TBV), cerebral cortex and white matter (WM), hippocampus, amygdale, pallidum, caudate, putamen, thalamus, accumbens, brain stem, cerebellum cortex and WM, lateral ventricles, inferior lateral ventricles, 3rd ventricle and 4th ventricle. All segmentations were manually inspected for accuracy by an experienced operator, and corrected in case of errors. Minor manual edits were performed on most participants (> 80%), usually restricted to removal of non-brain tissue, typically dura/ vessels adjacent to the cortex. Additionally, presence of local artefacts sometimes caused small parts of WM to be segmented as GM. Such errors were routinely corrected. For 21 participants, the final segmentations were judged to be of insufficient quality, and these were thus excluded from all analyses, reducing the sample from an initial 1121 to the reported 1100.

Intracranial volume (ICV) was estimated by use of an atlas-based normalization procedure, where the atlas scaling factor is used as a proxy for ICV, shown to correlate highly with manually derived ICV (r = .93) (Buckner et al., 2004). In a previous publications with an overlapping sample pool, the results for the pooled samples were replicable in each of the subsamples (Fjell et al., 2009b, Walhovd et al., 2011), indicating that the sensitivity of detecting effects are upheld and the statistical power are increased manifold. Thus, we are convinced that the approach of pooling data from different samples yields valid results. Still, to remove any offset effects of scanner, all analyses were done on the residuals after scanner was regressed out (see Statistical analyses).

Longitudinal change was calculated by use of Quarc, previously demonstrated to be highly sensitive to longitudinal volumetric changes based on MRI (Holland & Dale, 2011; Holland et al., 2011). Two MPRAGEs at each time-point were averaged to increase the ANR and CNR. An increase in SNR/ CNR is expected to yield more accurate change estimates. Labeling was done as described in Fischl et al. (2002) with FreeSurfer 3.0.2.

2.4 Statistical analyses

To reduce the number of comparisons, mean values for left and right hemisphere were used in all ROI analyses. Analyses were performed on residuals after the effects of sample/ scanner and ICV were removed. ICV was regressed out to remove the effects of the slight age-differences in head size (r = -.12, $p < 10^{-4}$).

For the cross-sectional analyses, a nonparametric local smoothing model, the smoothing

spline, implemented in Matlab, was fitted to the data. We have previously shown that this

approach gives less biased solutions than the more commonly employed higher-order

polynomial functions (Fjell et al., 2010a), and that caution should be exerted in inferring

trajectories from global fit models, e.g. the quadratic model. For instance, the peaks of

quadratic functions will inherently depend on the age range sampled. The quadratic function

is always a parabola, which sometimes causes the model to indicate a non-monotonous age-

relationship when non-linear but monotonous trajectories are a more likely. Also, for

quadratic models, the second derivative is assumed to be constant across the life span, and

hence the point of maximum acceleration of slope change cannot be determined.

We used an algorithm that optimizes smoothing level based on a version of Bayesian

Information Criterion (BIC), i.e. the smoothing level that minimizes BIC for each analysis was

chosen. BIC offers a relative measure of amount of information lost when a model is used to

describe a set of data, and thus describes the trade off between bias and variance in the

construction of models. BIC rewards goodness of fit, but includes a penalty that is an

increasing function of the number of estimated parameters. Thus, BIC attempts to find the

model that best explains the data with a minimum of free parameters, i.e. with a largest

possible smoothing level. With no smoothing, the smoothing spline will yield an extremely

good apparent fit to the data, but the model would not be generalizable (over-fitting). BIC

takes this into account by penalizing for loss of degrees of freedom. As BIC contains scaling

constants, the absolute BIC values are irrelevant. To ease comparison of BIC between

Ordinary Least Squares (OLS) linear models and smoothing spline models, we used Δ_I, which

is the difference between BIC for the model and the lowest BIC - in this case, the difference

between the smoothing spline model and the linear OLS model. As a rule of thumb, $\Delta_l \leq 2$

would indicate that the two models are essentially indistinguishable with regard to goodness

of fit, $\Delta_l \geq 4$ would indicate considerable differences between the models, and $\Delta_l \geq 10$ would

indicate that the linear model has essentially no support.

We calculated the ages where the slope of the local smoothing curve changed (the second

derivative), using the expression $-\dfrac{d^2 f(age)}{d\,age^2}$. We named these age-points critical ages, and

identified zero, one or two critical ages for each brain structure.

There were no clear differences in age distribution across samples (see Supplementary

Figure 1). Still, to avoid possible bias resulting from uneven age-distribution across samples

that could not be resolved by regressing out linear effects of sample and scanner, the main

smoothing spline analyses were also run for the main structures in a subset of participants

without any sample × age interaction. For each sample, an equal number of participants

were chosen for each decade, before the data were pooled. This sample included 522

participants, with a perfect distribution of participants across decades and samples.

For the longitudinal analyses, annual percentage change was calculated for each ROI. These

results have previously been reported (Fjell et al., 2009a), but was included to allow direct

comparison with the cross-sectional results. Correspondence between longitudinal data and

the smoothing spline models based on the cross-sectional data was assessed in two ways.

First, we tested whether the structures or regions that showed increases or decreases in the

full cross-sectional sample also showed longitudinal increases or decreases, respectively, in the independent ADNI sample. Second, we tested to what extent the pattern of estimated change across structures was the same in the cross-sectional and the longitudinal data. Unfortunately, the ADNI database contains only data for the latter part of the age-range (60-91 years), so comparisons with the cross-sectional results cannot be done throughout the adult life-span. Because the methods used to calculate longitudinal change and to fit the cross-sectional trajectories differ in important aspects, and the samples do not overlap, direct comparisons of estimations of absolute rates of atrophy between the longitudinal and cross-sectional results were not performed. Longitudinal reductions were measured as proportion of change between time points, and further converted to annual percentage volume change. Brain volumes in the cross-sectional data were regressed on sample and ICV, and age-reductions estimated from the cross-sectional data were measured in standard deviation decline in volume in the age-range 60 to 90.

3. Results

3.1 Cross-sectional data

To compare the linear and the smoothing spline models, we calculated BIC for the relationship between each brain volume and age (Supplementary Table 2, also including the quadratic model for comparison purposes). Scatterplots illustrating the estimated trajectories are presented in Figure 1 (structures) and Figure 2 (ventricular system). Of the 17 tested regions, a non-linear model represented the data best for 13 (total brain volume, cerebral cortex and WM, hippocampus, caudate, cerebellar WM, brain stem, pallidum, putamen, and lateral, inferior lateral, 3rd and 4th ventricle). The linear model showed the

best fit for five regions (nucleus accumbens, cerebellar cortex, amygdala, thalamus). For the putamen, BIC indicated that the smoothing spline model was marginally better than a linear model (BIC = 4.16), but deviation from linearity was minute. To test the stability of the results, a split half analysis was performed for WM volume (Supplementary Figure 2), yielding identical spline curves.

Inspections of the plots revealed substantial differences in estimated trajectories for the non-linear models. Especially, there were large differences in curvature. For some structures, there was a peak or an inflection point after which the age-relationship increased in strength (cerebral and cerebellar WM and hippocampus, to some degree TBV and the brainstem). For cerebral WM was a non-monotonous, inverse U-shaped relationship observed. For other structures, advanced age was accompanied by reduction in estimated change (caudate and all ventricular cavities, to some degree cerebral cortex and pallidum). Validation analyses in the subset of participants perfectly distributed across decades in all samples confirmed the results (Supplementary Figure 3).

[Insert Figure 1 and Figure 2 about here]

For the structures that showed deviations from linearity (except putamen), critical ages, i.e. the ages where estimated atrophy started to accelerate or decelerate, were identified. For some structures, one critical age was identified, while two were found for others (referred to as early and late critical age, see Figure 3). Early critical age varied greatly across structures, from 31 to 59 years, and volume-age correlations differed between the defined periods. For

the regions best described by a linear fit, age-correlations were as follows: amygdala r = -.56,

putamen r = -.69, thalamus r = -.65, nucleus accumbens r = -.70 and cerebellum GM r = -.52.

[Insert Figure 3 about here]

3.2 Longitudinal validation

All ROIs showed significant longitudinal change at p < .05. This confirmed the finding of

substantial atrophy/ ventricular expansion observed cross-sectionally for all ROIs, except the

caudate nucleus. For caudate, a weak positive correlation with age was observed after 59

years in the cross-sectional data, which was not found in the longitudinal analyses.

Next, we studied how well the pattern of cross-sectionally estimated change matched the

longitudinal findings. In the age-range 60-90 years, Spearman ρ between the cross-sectional

estimate of shrinkage and the longitudinally measured volume loss was .91 (p < 10^{-5}). In the

cross-sectional analyses, the regions with the steepest estimated decline between 60 and 90

were cerebral WM (z = -2.20), hippocampus (z = -2.05), cerebellum WM (z = -1.29) and

thalamus (z = -1.14). In the longitudinal analyses, the hippocampus showed the fastest

shrinkage rate (-0.83% annually), followed by amygdala (-0.81%), thalamus (-0.69%), cerebral

WM (-0.58%), accumbens and cerebellum WM (-0.57%), putamen (-0.43%), pallidum (-

0.40%), cerebellar cortex (-0.35%), the brainstem (-0.31%) and the caudate (-0.24%). For the

ventricles, there was perfect overlap between the cross-sectionally and longitudinally

estimated expansion, in that the inferior lateral ventricles (cross-sectionally estimated z =

2.92/ vs. longitudinally estimated % annual change = 5.47) showed the largest effects,

followed by the lateral ventricles (z = 2.15 vs. 4.40%), the 3rd ventricle (z = 1.8 vs. 3.07%) and

the 4th ventricle (z = 0.59 vs. 0.71%). Thus, although there was not a one-to-one

correspondence between the pattern of change across structures from the large cross-

sectional sample and the longitudinal sample, there was still substantial overlap.

4. Discussion

There were three main findings: First, a heterogeneous pattern of discontinuous age-

correlations in different age-spans characterised the majority of brain regions, and critical

ages for changes in estimated rates of atrophy could be identified. Second, accelerated

estimated reduction with advanced age is not the norm of brain aging. Rather, different

structures showed a mix of trajectories. When more negative (positive for CSF) age-volume

correlations were seen in the last part of the age-span, this would typically start in mid-life.

Finally, the longitudinal analyses in general supported the cross-sectional results, with a

reasonably coherent pattern of atrophy across structures.

4.1 Trajectories of estimated change across the adult life-span

Cross-sectional studies have shown non-linear age-relationships for the volume of several

brain structures (Raz et al., 2004, Allen et al., 2005, Lupien et al., 2007), including studies

with samples overlapping the present (Walhovd et al., 2009). There have, however, been

few attempts to describe the trajectories in detail (for exceptions, see (Jernigan et al., 2001b,

Fjell et al., 2010a, Schuff et al., 2010)). We identified three basic types of trajectories:

(1) Linear reduction: Amygdala, putamen, thalamus, accumbens and the cerebellar cortex were all linearly related to age (all r's < -.52), confirming previous findings (Gunning-Dixon et al., 1998, Jernigan et al., 2001a, Allen et al., 2005, Curiati et al., 2009, Walhovd et al., 2011).

(2) Stability followed by decline: Hippocampus, the brain stem and cerebellar WM exhibited initial weak age-correlations, but with acceleration of estimated decline from around mid-life. Hippocampus is especially important due to its role in memory and early AD (de Leon et al., 2006, Du et al., 2007, Jack et al., 2008, Fennema-Notestine et al., 2009, McEvoy et al., 2009). Cross-sectional studies have shown prolonged development (Ostby et al., 2009) and a marked non-linear pattern of estimated change in adulthood (Allen et al., 2005, Jernigan and Gamst, 2005, Walhovd et al., 2005, Kennedy et al., 2008, Fjell et al., 2010a). We found that after a period of relative stability during mid-life, accelerated estimated reductions started at about 50 years of age, followed by a strongly negative linear age-relationship from 60 years. Cerebral WM was the only structure positively correlated with age in the earliest part of the age-range, followed by a strong negative relationship. This pattern is in line with a previous publication reporting multi-modal imaging data from 8-85 years, partly overlapping sample five (Westlye et al., 2010b). The ventricles showed modest estimated increase or slow decrease until 50-60 years, followed by steep estimated expansion during the last phase of life.

(3) Steep, non-linear decline: Total brain volume (TBV), cerebral cortex and pallidum showed two critical ages with slight differences in estimated decline. TBV correlated stronger with age after 60 years than in the preceding life-phases (p < .05, by use of t-tests of Fisher's z-transformed correlations). In contrast, pallidum and the cerebral cortex correlated stronger with age early (p < .05).

Caudate was the most deviant structure, best described by a U-shaped trajectory. We advise to interpret this with great caution, however, as this result was not in coherence with the longitudinal analyses, and we have no reason to expect an increase in volume in the latter part of the life-span.

4.2 Critical ages in estimated regional brain change

The trajectory of a neuroanatomical volume across age represents the additive combination of several neurobiological processes. We suggest that changes in the relative impact of these can be observed as turning points in the estimated change in brain volumes, what we refer to as critical ages (see Figure 4). For instance, WM increases in volume well into adulthood (Pfefferbaum et al., 1994, Giedd, 2004, Wozniak and Lim, 2006, Westlye et al., 2010b), with myelination being one likely underlying factor. After mid-life, volume decreases (Allen et al., 2005, Walhovd et al., 2011), likely partly caused by loss of small myelinated fibers and myelin breakdown (Meier-Ruge et al., 1992, Peters et al., 2000). This will be affected by medical conditions such as hypertension, cholesterol, diabetes or metabolic syndrome, genetic variations such as apolipoprotein E (APOE), and variables such as cognitive activity and education. Processes with opposite effects on WM volume probably work concurrently, e.g. redundant myelination (Peters et al., 2000) and fluid bubbles in the myelin sheet with higher age (Peters and Sethares, 2002). The relative impact of each of these processes likely changes across the age-span. To speculate, one scenario may be as follows: The additive effects of developmental processes cause the observed WM volume growth in the first half of the age-span. However, after a certain age, myelin breakdown and loss of small

myelinated fibers play increasingly important roles, likely before the developmental

processes have come to an end. Eventually, the degenerative processes will impact the WM

volume to such an extent that yearly growth is no longer linear, but is gradually reduced. At

this point, the second derivative of the age-volume trajectory will change, representing a

critical age. As such, the estimated volume of a brain structure alone reflects the sum of

many concurrent developmental and degenerative biological processes. We believe that

identification of turning points may add to our understanding of the trajectories of brain

volumes across the adult life-span. The trajectory depicted in Figure 4 is meant to illustrate

the principle of how accumulated influence of opposing factors affects volume, but is not

intended to accurately depict the life-course of any single structure.

[Insert Figure 4 about here]

The differences in the slope of the curves between the critical ages varied greatly between

structures. While the cerebral cortex was almost linearly related to age, cerebral WM and

the hippocampus showed large slope differences in the age-ranges on each side of the

critical age. Although not estimated in the present study, confidence intervals for the critical

ages will likely be larger for the more linear slopes than for the distinct non-linear and even

non-monotonous slopes.

4.3 Cross-sectional vs. longitudinal results

It is impossible to infer changes in brain structures based on cross-sectional data alone (Raz

and Lindenberger, 2010), as this depends on assumptions of no cohort-effects and selection

bias. These assumptions may generally not be valid and cross-sectional estimates of change diverge substantially (Raz et al., 2005), and sometimes even oppose longitudinal observations (Nyberg et al., 2010, Raz and Lindenberger, 2011). Therefore, longitudinal data from an independent sample (Fjell et al., 2009a) were included in the present paper. With the exception of caudate volume, the direction and statistical significance of the age-relationships in the cross-sectional data were confirmed by the longitudinal analyses. Further, although far from perfect, there was a reasonably coherent relationship between the pattern of atrophy between cross-sectional and longitudinal results: the structures with the largest age-correlations in the cross-sectional material tended to show the highest rates of annual atrophy/ expansion. The rank-order correlation was .91. Thus, at least in their rank order of magnitude, the cross-sectional results for the age-range above 60 years seem to be largely in coherence with independent longitudinal data.

Nonetheless, caution must still be exercised in interpreting the results, as longitudinal data were available for the oldest part of the sample only. The observed correlation between age and ICV indicates that cohort differences may indeed exist in the sample. Still, age accounted for only 1.4% of the variance in ICV, and all analyses were performed on residuals after ICV was regressed out. As the main determinant of ICV is the lifetime maximum size of the brain, ICV-corrections reduce the impact of cohort effects. Some evidence even suggests that cross-sectional studies may underestimate the extent of regional brain shrinkage in some regions (Raz et al., 2005).

Of more general concern is that the inherent problem of mapping life-span trajectories from cross-sectional examinations cannot easily be resolved with longitudinal data, since longitudinal examinations of brain structures over decades are not feasible, and longitudinal studies have methodological problems of their own (e.g. selective recruitment and attrition). Adding to this, most longitudinal studies are limited in age-span, sample size and number of follow-ups. To some degree, combined cross-sectional and longitudinal designs can alleviate the concerns raised above. For instance, accelerated hippocampal atrophy with age has been demonstrated (Raz et al., 2005, Driscoll et al., 2009, Fjell et al., 2009a, Raz et al., 2010). However, all of these studies except Raz et al. (2005) comprised middle-aged and elderly participants only, and the results thus inform us less about life-span trajectories.

It is important to keep in mind that brain volumes change within relatively narrow time windows. As long as we do not know the true shape of these processes, it is unclear how many critical turning points there are in brain development and aging. An ideal approach to reproduce the dynamic process of change would be longitudinal studies with high density of measures and assessment of multiple time windows across the life span (Raz et al., 2010; Raz & Lindenberger, 2011).

Several factors affect the estimated trajectories at the group level and the actual trajectories at the individual level. These include genetic variations such as APOE, and medical factors such as hypertension, cholesterol and diabetes (for a review, see e.g. Raz et al., 2012). In addition, cognitive activity or training may impact brain structure even in older age (Zatorre et al., 2012). Future studies should further explore the impact and interactions between

genetic, environmental and medical factors on brain structure throughout the adult life. More knowledge about these processes will increase our understanding of normal brain aging. Also, possible influence of pre-symptomatic Alzheimer's disease (AD) can be difficult to disentangle from normal age-changes in the older participants, as follow-up examinations over several years are necessary to exclude subjects with incipient disease. However, while this factor is difficult to completely rule out from the present results, there are indications that this is not likely to have affected the trajectories to a substantial degree. Even though hippocampal volume is the structure that distinguishes best between AD-patients and healthy elderly, amygdala is also affected in early stages of the disease (Fjell et al., 2010b). While the age-slope for hippocampus is much steeper after 60 years, this is not seen for amygdala, which would be expected if incipient AD was a major factor in shaping the estimated trajectories. Even if a few of the participants had incipient AD and consequently abnormal volume decline in select structures, the smoothing spline approach is relatively robust to the influence of outliers as long as the sample size is large.

4.4 Conclusion

The present study shows that the majority of brain structures follow complex, non-linear volumetric trajectories through adult life. Important next step to increased understanding of the mechanisms of brain aging will be to conduct large-scale, multi-modal imaging studies, combining e.g. volumetry, DTI and intensity/contrast measures (Fjell et al., 2008, Westlye et al., 2010b, a), as well as longitudinal studies with high density of measurements to examine the trajectories across age with regards to the critical phases proposed on the basis of the cross-sectional analyses.

5. Acknowledgement

are disseminated by the Laboratory of Neuro Imaging at the University of California, Los

Angeles.

6. **References**

Abe O, Yamasue H, Aoki S, Suga M, Yamada H, Kasai K, Masutani Y, Kato N, Kato N, Ohtomo K. 2008. Aging in the CNS: Comparison of gray/white matter volume and diffusion tensor data. Neurobiol Aging 29:102-116.

Alexander GE, Chen K, Merkley TL, Reiman EM, Caselli RJ, Aschenbrenner M, Santerre-Lemmon L, Lewis DJ, Pietrini P, Teipel SJ, Hampel H, Rapoport SI, Moeller JR. 2006. Regional network of magnetic resonance imaging gray matter volume in healthy aging. Neuroreport 17:951-956.

Allen JS, Bruss J, Brown CK, Damasio H. 2005. Normal neuroanatomical variation due to age: the major lobes and a parcellation of the temporal region. Neurobiol Aging 26:1245-1260; discussion 1279-1282.

Buckner RL, Head D, Parker J, Fotenos AF, Marcus D, Morris JC, Snyder AZ. 2004. A unified approach for morphometric and functional data analysis in young, old, and demented adults using automated atlas-based head size normalization: reliability and validation against manual measurement of total intracranial volume. NeuroImage 23:724-738.

Curiati PK, Tamashiro JH, Squarzoni P, Duran FL, Santos LC, Wajngarten M, Leite CC, Vallada H, Menezes PR, Scazufca M, Busatto GF, Alves TC. 2009. Brain structural variability due to aging and gender in cognitively healthy Elders: results from the Sao Paulo Ageing and Health study. AJNR Am J Neuroradiol 30:1850-1856.

de Leon MJ, DeSanti S, Zinkowski R, Mehta PD, Pratico D, Segal S, Rusinek H, Li J, Tsui W, Saint Louis LA, Clark CM, Tarshish C, Li Y, Lair L, Javier E, Rich K, Lesbre P, Mosconi L, Reisberg B, Sadowski M, DeBernadis JF, Kerkman DJ, Hampel H, Wahlund LO, Davies

P. 2006. Longitudinal CSF and MRI biomarkers improve the diagnosis of mild cognitive impairment. Neurobiol Aging 27:394-401.

Driscoll I, Davatzikos C, An Y, Wu X, Shen D, Kraut M, Resnick SM. 2009. Longitudinal pattern of regional brain volume change differentiates normal aging from MCI. Neurology 72:1906-1913.

Du AT, Schuff N, Kramer JH, Rosen HJ, Gorno-Tempini ML, Rankin K, Miller BL, Weiner MW. 2007. Different regional patterns of cortical thinning in Alzheimer's disease and frontotemporal dementia. Brain 130:1159-1166.

Fennema-Notestine C, Hagler DJ, Jr., McEvoy LK, Fleisher AS, Wu EH, Karow DS, Dale AM. 2009. Structural MRI biomarkers for preclinical and mild Alzheimer's disease. Hum Brain Mapp 30:3238-3253.

Fischl B, Salat DH, Busa E, Albert M, Dieterich M, Haselgrove C, van der Kouwe A, Killiany R, Kennedy D, Klaveness S, Montillo A, Makris N, Rosen B, Dale AM. 2002. Whole brain segmentation: automated labeling of neuroanatomical structures in the human brain. Neuron 33:341-355.

Fischl B, Salat DH, van der Kouwe AJ, Makris N, Segonne F, Quinn BT, Dale AM. 2004. Sequence-independent segmentation of magnetic resonance images. NeuroImage 23 Suppl 1:S69-84.

Fjell AM, Westlye LT, Grydeland H, Amlien I, Espeseth T, Reinvang I, Raz N, Dale AM, Walhovd KB. Accelerating Cortical Thinning: Unique dementia or Universal in Aging? Cereb Cortex, in press.

Fjell AM, Walhovd KB, Westlye LT, Ostby Y, Tamnes CK, Jernigan TL, Gamst A, Dale AM. 2010a. When does brain aging accelerate? Dangers of quadratic fits in cross-sectional studies. NeuroImage 50:1376-1383.

Fjell AM, Walhovd KB, Fennema-Notestine C, McEvoy LK, Hagler DJ, Holland D, Brewer JB, Dale AM. 2010b. CSF biomarkers in prediction of cerebral and clinical change in Mild Cognitive Impairment and Alzheimer 's disease. J Neuroscience: 10, 2088-2101.

Fjell AM, Walhovd KB, Fennema-Notestine C, McEvoy LK, Hagler DJ, Holland D, Brewer JB, Dale AM. 2009a. One-year brain atrophy evident in healthy aging. J Neurosci 29:15223-15231.

Fjell AM, Westlye LT, Amlien I, Espeseth T, Reinvang I, Raz N, Agartz I, Salat DH, Greve DN, Fischl B, Dale AM, Walhovd KB. 2009b. High consistency of regional cortical thinning in aging across multiple samples. Cereb Cortex 19:2001-2012.

Fjell AM, Westlye LT, Amlien I, Espeseth T, Reinvang I, Raz N, Agartz I, Salat DH, Greve DN, Fischl B, Dale AM, Walhovd KB. 2009c. Minute effects of sex on the aging brain: a multisample magnetic resonance imaging study of healthy aging and Alzheimer's disease. J Neurosci 29:8774-8783.

Fjell AM, Westlye LT, Greve DN, Fischl B, Benner T, van der Kouwe AJ, Salat D, Bjornerud A, Due-Tonnessen P, Walhovd KB. 2008. The relationship between diffusion tensor imaging and volumetry as measures of white matter properties. NeuroImage 42:1654-1668.

Folstein MF, Folstein SE, McHugh PR. 1975. "Mini-mental state". A practical method for grading the cognitive state of patients for the clinician. J Psychiatr Res 12:189-198.

Giedd JN. 2004. Structural magnetic resonance imaging of the adolescent brain. Ann N Y Acad Sci 1021:77-85.

Good CD, Johnsrude IS, Ashburner J, Henson RN, Friston KJ, Frackowiak RS. 2001. A voxel-based morphometric study of ageing in 465 normal adult human brains. NeuroImage 14:21-36.

Greenberg DL, Messer DF, Payne ME, Macfall JR, Provenzale JM, Steffens DC, Krishnan RR. 2008. Aging, gender, and the elderly adult brain: an examination of analytical strategies. Neurobiol Aging 29:290-302.

Gunning-Dixon FM, Head D, McQuain J, Acker JD, Raz N. 1998. Differential aging of the human striatum: a prospective MR imaging study. AJNR Am J Neuroradiol 19:1501-1507.

Holland D, Dale AM. 2011. Nonlinear registration of longitudinal images and measurement of change in regions of interest. Med Image Anal 15:489-497.

Holland D, McEvoy LK, Dale AM. 2011. Unbiased comparison of sample size estimates from longitudinal structural measures in ADNI. Human brain mapping.

Jack CR, Jr., Weigand SD, Shiung MM, Przybelski SA, O'Brien PC, Gunter JL, Knopman DS, Boeve BF, Smith GE, Petersen RC. 2008. Atrophy rates accelerate in amnestic mild cognitive impairment. Neurology 70:1740-1752.

Jernigan TL, Archibald SL, Fennema-Notestine C, Gamst AC, Stout JC, Bonner J, Hesselink JR. 2001a. Effects of age on tissues and regions of the cerebrum and cerebellum. Neurobiol Aging 22:581-594.

Jernigan TL, Archibald SL, Fennema-Notestine C, Gamst AC, Stout JC, Bonner J, Hesselink JR. 2001b. Effects of age on tissues and regions of the cerebrum and cerebellum. Neurobiol Aging 22:581-594.

Jernigan TL, Gamst AC. 2005. Changes in volume with age--consistency and interpretation of observed effects. Neurobiol Aging 26:1271-1274; discussion 1275-1278.

Kennedy KM, Erickson KI, Rodrigue KM, Voss MW, Colcombe SJ, Kramer AF, Acker JD, Raz N. 2008. Age-related differences in regional brain volumes: A comparison of optimized voxel-based morphometry to manual volumetry. Neurobiol Aging.

Lupien SJ, Evans A, Lord C, Miles J, Pruessner M, Pike B, Pruessner JC. 2007. Hippocampal volume is as variable in young as in older adults: implications for the notion of hippocampal atrophy in humans. NeuroImage 34:479-485.

McEvoy LK, Fennema-Notestine C, Roddey JC, Hagler DJ, Jr., Holland D, Karow DS, Pung CJ, Brewer JB, Dale AM, Alzheimer's Disease Neuroimaging I. 2009. Alzheimer disease: quantitative structural neuroimaging for detection and prediction of clinical and structural changes in mild cognitive impairment. Radiology 251:195-205.

Meier-Ruge W, Ulrich J, Bruhlmann M, Meier E. 1992. Age-related white matter atrophy in the human brain. Ann N Y Acad Sci 673:260-269.

Morris JC. 1993. The Clinical Dementia Rating. CDR): current version and scoring rules. Neurology 43:2412-2414.

Nunnemann S, Wohlschlager AM, Ilg R, Gaser C, Etgen T, Conrad B, Zimmer C, Muhlau M. 2007. Accelerated aging of the putamen in men but not in women. Neurobiol Aging.

Nyberg L, Salami A, Andersson M, Eriksson J, Kalpouzos G, Kauppi K, Lind J, Pudas S, Persson J, Nilsson LG. 2010. Longitudinal evidence for diminished frontal cortex function in aging. Proc Natl Acad Sci U S A 107:22682-22686.

Ostby Y, Tamnes CK, Fjell AM, Westlye LT, Due-Tonnessen P, Walhovd KB. 2009. Heterogeneity in subcortical brain development: A structural magnetic resonance imaging study of brain maturation from 8 to 30 years. The Journal of neuroscience : the official journal of the Society for Neuroscience 29:11772-11782.

Peters A, Moss MB, Sethares C. 2000. Effects of aging on myelinated nerve fibers in monkey primary visual cortex. J Comp Neurol 419:364-376.

Peters A, Sethares C. 2002. Aging and the myelinated fibers in prefrontal cortex and corpus callosum of the monkey. J Comp Neurol 442:277-291.

Pfefferbaum A, Mathalon DH, Sullivan EV, Rawles JM, Zipursky RB, Lim KO. 1994. A quantitative magnetic resonance imaging study of changes in brain morphology from infancy to late adulthood. Arch Neurol 51:874-887.

Raz N, Yang Y, Dahle CL, Land S. 2012. Volume of white matter hyperintensities in healthy adults: contribution of age, vascular risk factors, and inflammation-related genetic variants. Biochim Biophys Acta 1822: 361-369.

Raz N, Ghisletta P, Rodrigue KM, Kennedy KM, Lindenberger U. 2010. Trajectories of brain aging in middle-aged and older adults: regional and individual differences. NeuroImage 51:501-511.

Raz N, Gunning-Dixon F, Head D, Rodrigue KM, Williamson A, Acker JD. 2004. Aging, sexual dimorphism, and hemispheric asymmetry of the cerebral cortex: replicability of regional differences in volume. Neurobiol Aging 25:377-396.

Raz N, Lindenberger U. 2010. News of cognitive cure for age-related brain shrinkage is premature: a comment on Burgmans et al.. 2009). Neuropsychology 24:255-257.

Raz N, Lindenberger U. 2011. Only time will tell: cross-sectional studies offer no solution to the age-brain-cognition triangle: comment on Salthouse. 2011). Psychol Bull 137:790-795.

Raz N, Lindenberger U, Rodrigue KM, Kennedy KM, Head D, Williamson A, Dahle C, Gerstorf D, Acker JD. 2005. Regional brain changes in aging healthy adults: general trends, individual differences and modifiers. Cereb Cortex 15:1676-1689.

Raz N, Rodrigue KM. 2006. Differential aging of the brain: patterns, cognitive correlates and modifiers. Neurosci Biobehav Rev 30:730-748.

Raz N, Rodrigue KM, Kennedy KM, Dahle C, Head D, Acker JD. 2003. Differential age-related changes in the regional metencephalic volumes in humans: a 5-year follow-up. Neurosci Lett 349:163-166.

Schuff N, Tosun D, Insel PS, Chiang GC, Truran D, Aisen PS, Jack CR, Jr., Weiner MW. 2010. Nonlinear time course of brain volume loss in cognitively normal and impaired elders. Neurobiology of aging.

Smith SM, Johansen-Berg H, Jenkinson M, Rueckert D, Nichols TE, Miller KL, Robson MD, Jones DK, Klein JC, Bartsch AJ, Behrens TE. 2007. Acquisition and voxelwise analysis of multi-subject diffusion data with tract-based spatial statistics. Nat Protoc 2:499-503.

Sullivan EV, Marsh L, Mathalon DH, Lim KO, Pfefferbaum A. 1995. Age-related decline in MRI volumes of temporal lobe gray matter but not hippocampus. Neurobiol Aging 16:591-606.

Sullivan EV, Rosenbloom M, Serventi KL, Pfefferbaum A. 2004. Effects of age and sex on volumes of the thalamus, pons, and cortex. Neurobiol Aging 25:185-192.

Walhovd KB, Fjell AM, Reinvang I, Lundervold A, Dale AM, Eilertsen DE, Quinn BT, Salat D, Makris N, Fischl B. 2005. Effects of age on volumes of cortex, white matter and subcortical structures. Neurobiol Aging 26:1261-1270; discussion 1275-1268.

Walhovd KB, Westlye LT, Amlien I, Espeseth T, Reinvang I, Raz N, Agartz I, Salat DH, Greve DN, Fischl B, Dale AM, Fjell AM. 2011. Consistent neuroanatomical age-related volume differences across multiple samples. Neurobiol Aging 32:916-932.

Westlye LT, Walhovd KB, Dale AM, Bjornerud A, Due-Tonnessen P, Engvig A, Grydeland H, Tamnes CK, Ostby Y, Fjell AM. 2010a. Differentiating maturational and aging-related changes of the cerebral cortex by use of thickness and signal intensity. NeuroImage 52:172-185.

Westlye LT, Walhovd KB, Dale AM, Bjornerud A, Due-Tonnessen P, Engvig A, Grydeland H, Tamnes CK, Ostby Y, Fjell AM. 2010b. Life-span changes of the human brain white matter: diffusion tensor imaging. DTI. and volumetry. Cereb Cortex 20:2055-2068.

Westlye LT, Walhovd KB, Dale AM, Espeseth T, Reinvang I, Raz N, Agartz I, Greve DN, Fischl B, Fjell AM. 2009. Increased sensitivity to effects of normal aging and Alzheimer's disease on cortical thickness by adjustment for local variability in gray/white contrast: a multi-sample MRI study. NeuroImage 47:1545-1557.

Wozniak JR, Lim KO. 2006. Advances in white matter imaging: a review of in vivo magnetic resonance methodologies and their applicability to the study of development and aging. Neurosci Biobehav Rev 30:762-774.

Zatorre RJ, Fields RD, Johansen-Berg H. 2012. Plasticity in gray and white: neuroimaging

changes in brain structure during learning. Nat Neurosci 18: 528-536.

Figure legends

Figure 1 Scatterplots of age-brain structure relationships

The figure shows the individual data points and the cross-sectionally estimated trajectories

for the 13 brain structures of interest based on the smoothing spline. Y-axis values represent

mean volume across hemispheres, corrected for the influence of sample and intracranial

volume (Z-scores). The right bottom figure shows some of the segmented structures of the

average brain of Sample 2. The three-dimensional renderings illustrate the average shape,

extension and relative position within the brain. The cerebral cortex and underlying white

matter are made transparent to allow visualization of the underlying subcortical structures.

Figure 2 Scatterplots of age - ventricular system relationships

The figure shows the individual data points and the cross-sectionally estimated trajectories

for the ventricles based on the smoothing spline. Y-axis values represent mean volume

across hemispheres, corrected for the influence of sample and intracranial volume (Z-

scores).

Figure 3 Estimated age-trajectories and critical ages

The figure shows the estimated age-trajectories from the cross-sectional analyses for the 12

areas that deviated from linearity, based on the smoothing spline. Critical ages, identified by

changes in the second derivative, are displayed. Pearson correlations between brain volume

and age are shown for each age phase separated by the critical ages. All correlations were

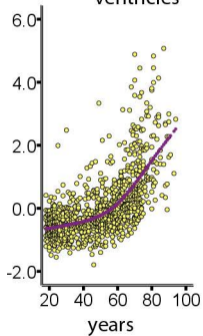significant at $p < .05$, except for pallidum in middle age (.01), cerebellum WM in young age (-

.02) and brain stem in young age (.01). Due to small age-variance, correlations are not presented for age-phases defined by critical ages of 80 years or higher. Critical ages are indicative of phases where estimated changes in brain volumes are in transitions.

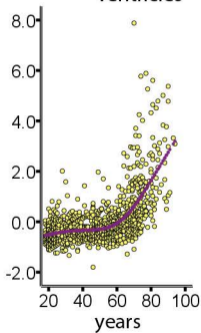**Figure 4 A hypothetic model for discontinuous change in rate of atrophy**

The figure represents a simplified attempt to visualize how two sets of age-dependent degenerative effects can affect the age-trajectory of a brain volume, and how timing of critical ages reflect the start and endpoint of these effects. The blue line represents the volume of a brain structure through life, e.g. WM volume. In the first part of life, volume increases, caused by the sum of progressive events, e.g. myelination and axonal growth (green line). Before the maturational changes caused by the progressive events have come to an end, degenerative events starts, e.g. selective loss of small-diameter myelinated axons (primary degenerative event) and demyelination of larger connections (secondary degenerative event). The onset of these processes will affect the growth rate of the curve, detected as a change in the second derivative, and this change can be termed early critical age. After this point, the volume increase slowly decelerates. After continuous impact on the volume from these two processes, one of them eventually burns out in higher age while the other continues further. This causes a late critical age, where the volume reductions slowly starts to level off. This is of course a gross simplification of the processes in the brain and the trajectories that may characterize them. The main point is to illustrate that critical ages may be used in the characterisation of estimated age-trajectories of brain volumes, and that they may be related to underlying neurobiological events, both developmental and degenerative.
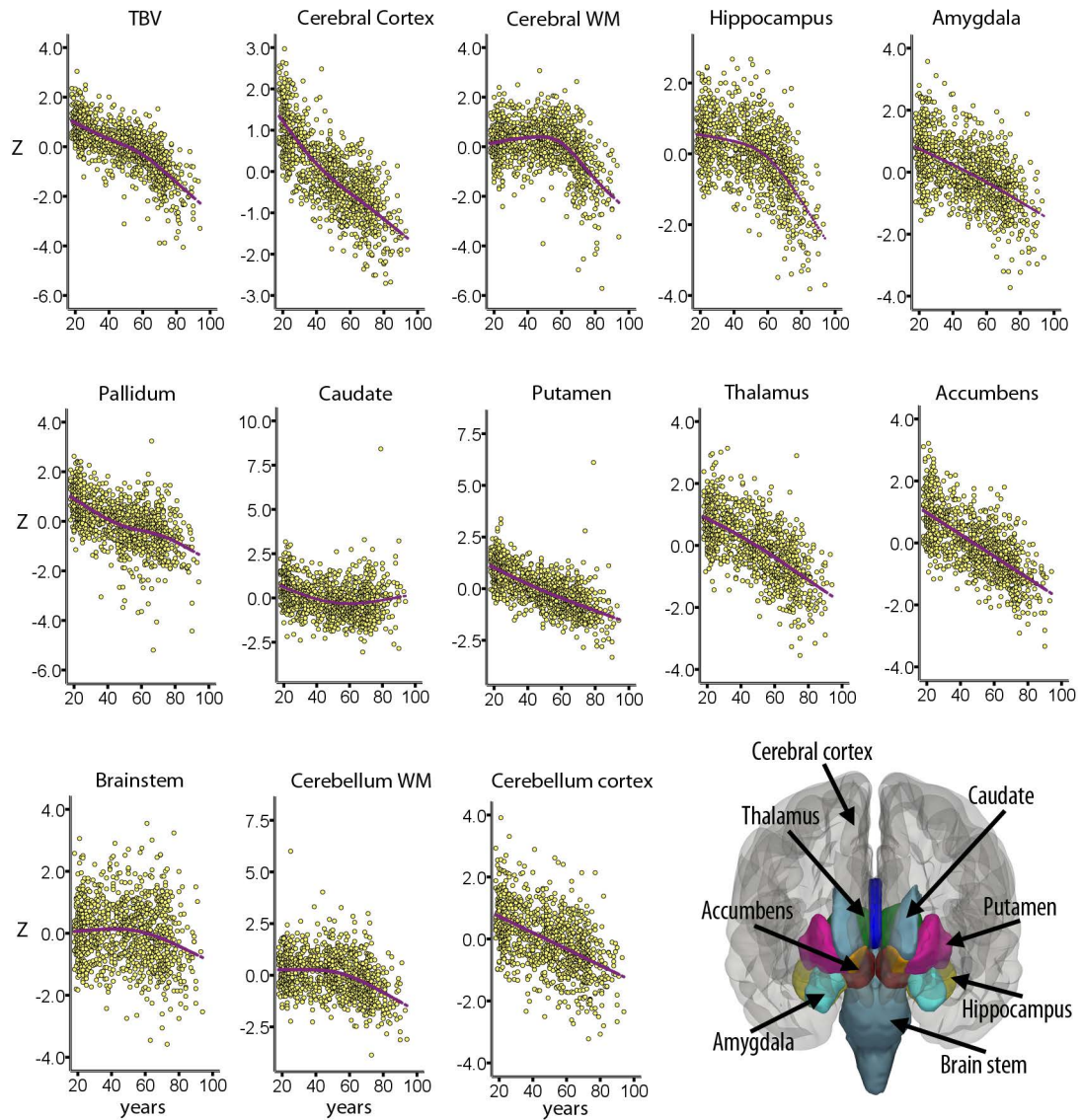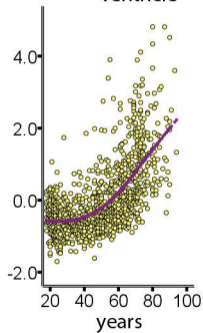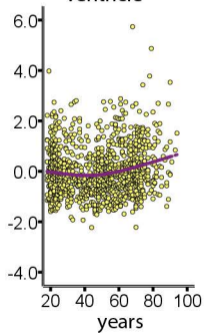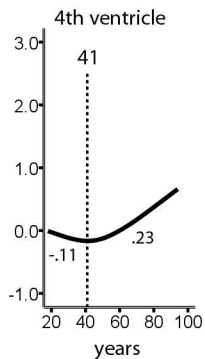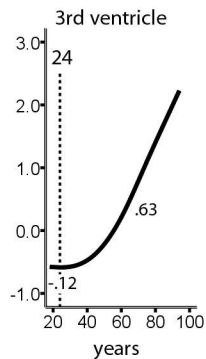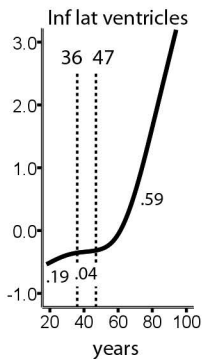
| Lateral ventricles | Inferior lateral ventricles | 3rd ventricle | 4th ventricle |

Z vs years

	Critical Age: Early		Critical Age: Late	

Developmental events

Volume

Primary degenerative events

Secondary degenerative events

25 50 75 100

Year

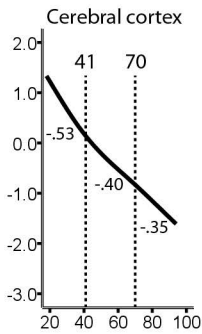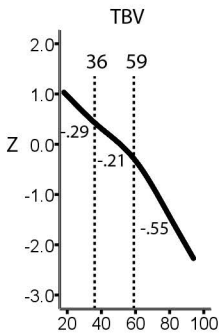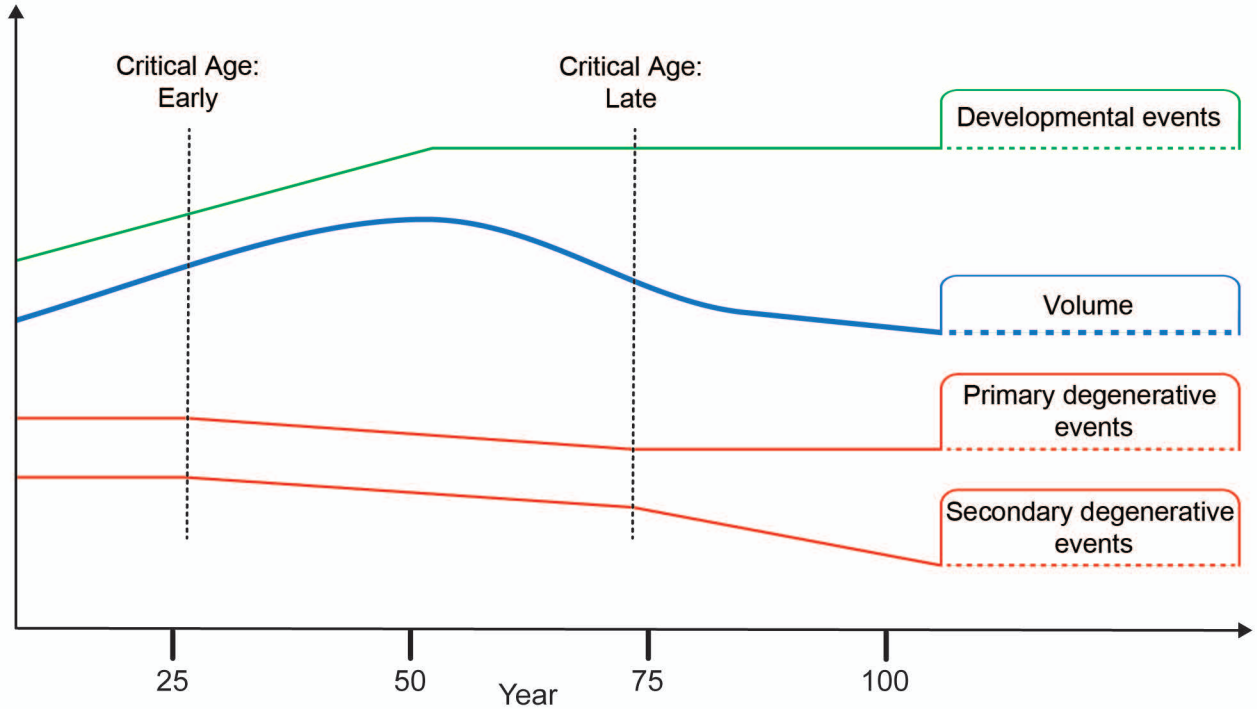| Sample	Country	N (% f)	Age mean (range)	Education mean (range)	Key publications	Main screening instruments/ inclusion criteria
1	Norway	69 (57)	51.3 (20-88)	15 (7-20)	(Walhovd et al., 2005a)	Health interview, MMSE > 26, BDI < 16, IQ > 85, RH only
2	Norway	208 (71)	46.8 (19-75)	14 (9-22)	(Espeseth et al., 2008)	Health interview, IQ > 85
3	USA	309 (63)	44.5 (18-94)	3.5 (1-5)[c]	(Marcus et al., 2007)	Health interview, CDR = 0[b], MMSE > 25[b], RH only
4	USA	191 (60)	47.3 (18-81)	15.7 (12-21)	(Raz et al., 2004a)	Health interview, BIMCT > 30, GDQ < 15, RH only, neuroradiology,
5	Norway	323 (57)	50.8 (20-85)	15.6[e] (4-26)	(Fjell et al., 2010; Westlye et al., 2010)	Health interview, Neuropsychological evaluation, BDI < 16, IQ > 85, RH only

Nor: Norway

% f: percentage of female participants

MMSE: Mini Mental Status Exam (Folstein et al. 1975)

BDI: Beck Depression Inventory (Beck, 1987)

BIMCT: Blessed Information-Memory-Concentration Test (Blessed et al. 1968)

CDR: Clinical Dementia Rating (Berg, 1984, 1988; Morris, 1993)

GDQ: Geriatric Depression Questionnaire (Auer and Reisberg, 1997)

RH: Right handed

WASI: Wechsler Abbreviated Scale of Intelligence (Wechsler, 1999)

[a] Available for 70 participants

[b] Available for participants $\geq$ 60 years only

[c] Available for all participants $\geq$ 60 years, and sporadically for the rest. 1: less than high school grad., 2: high school grad., 3: some college, 4: college grad., 5: beyond college

[d] Alzheimer patients

[e] Missing for four participant

Table 1 Sample characteristics cross-sectional sample

Structure	Linear BIC	Quadratic BIC	Smoothing spline BIC	Linear vs smoothing Δ BIC
Total Brain Volume	32165.77	32142.15	32134.01	**31.76**
Cerebral cortex	32006.13	31984.60	31980.57	**25.56**
Cerebral WM	7548.20	7370.2	7360.08	**188.12**
Hippocampus	7327.24	7227.79	7226.24	**101**
Amygdala	7302.48	7301.69	7301.17	1.31
Pallidum	7301.54	7298.56	7289.19	**12.35**
Caudate	7623.18	7564.97	7570.50	**52.68**
Putamen	6999.88	6996.99	6995.72	**4.16**
Thalamus	7105.95	7104.36	7103.14	2.81
Accumbens	6981.52	6988.51	6981.56	-0.04
Brain stem	33020.28	33001.76	33003.99	**16.29**
Cerebellum cortex	7362.42	7369.39	7362.46	-0.04
Cerebellum WM	7594.55	7548.38	7550.45	**44.1**
Ventricles				
Lateral ventricles	7145.50	7015.81	7011.87	**133.63**
Inf Lat Vent	32636.83	32424.91	32385.02	**251.81**
3rd ventricle	32502.03	32386.94	32387.29	**114.74**
4th ventricle	33024.24	33006.05	33007.41	**16.83**

Table 2 Testing of linearity

Δ BIC > 4 indicates that the smoothing spline modell yield a better account of the data than the linear modell, while BIC $\leq$ 4 indicates that a liner fit to the data are the most appropriate. BIC values for the quadratic model are included for comparison purposes.

Bold indicates BIC $\leq$ 4

BIC: Bayesian Information Criterion

Sample	Country	N (% f)	Age mean (range)	Education mean (range)	Key publications	Main screening instruments/ inclusion criteria
1	Norway	69 (57)	51.3 (20-88)	15 (7-20)	(Walhovd et al., 2005a)	Health interview, MMSE > 26, BDI < 16, IQ > 85, RH only
2	Norway	208 (71)	46.8 (19-75)	14 (9-22)	(Espeseth et al., 2008)	Health interview, IQ > 85
3	USA	309 (63)	44.5 (18-94)	3.5 (1-5)[c]	(Marcus et al., 2007)	Health interview, CDR = 0[b], MMSE > 25[b], RH only
4	USA	191 (60)	47.3 (18-81)	15.7 (12-21)	(Raz et al., 2004a)	Health interview, BIMCT > 30, GDQ < 15, RH only, neuroradiology,
5	Norway	323 (57)	50.8 (20-85)	15.6[e] (4-26)	(Fjell et al., 2010; Westlye et al., 2010)	Health interview, Neuropsychological evaluation, BDI < 16, IQ > 85, RH only

Nor: Norway

% f: percentage of female participants

MMSE: Mini Mental Status Exam (Folstein et al. 1975)

BDI: Beck Depression Inventory (Beck, 1987)

BIMCT: Blessed Information-Memory-Concentration Test (Blessed et al. 1968)

CDR: Clinical Dementia Rating (Berg, 1984, 1988; Morris, 1993)

GDQ: Geriatric Depression Questionnaire (Auer and Reisberg, 1997)

RH: Right handed

WASI: Wechsler Abbreviated Scale of Intelligence (Wechsler, 1999)

[a] Available for 70 participants

[b] Available for participants $\geq$ 60 years only

[c] Available for all participants $\geq$ 60 years, and sporadically for the rest. 1: less than high school grad., 2: high school grad., 3: some college, 4: college grad., 5: beyond college

[d] Alzheimer patients

[e] Missing for four participant

Supplemental Table 1 Sample characteristics cross-sectional sample

Structure	Linear	Smoothing spline	Linear vs smoothing
	BIC	BIC	Δ BIC
Total Brain Volume	32166	32134	**32**
Cerebral cortex	32006	31981	**25**
Cerebral WM	7548	7360	**188**
Hippocampus	7327	7226	**101**
Amygdala	7302	7301	1
Pallidum	7302	7289	**13**
Caudate	7623	7571	**52**
Putamen	7000	6996	**4**
Thalamus	7106	7103	3
Accumbens	6982	6982	0
Brain stem	33020	33004	**16**
Cerebellum cortex	7362	7362	0
Cerebellum WM	7595	7550	**44**
Ventricles			
Lateral ventricles	7146	7012	**134**
Inf Lat Vent	32637	32385	**252**
3rd ventricle	32502	32387	**115**
4th ventricle	33024	33007	**17**

Supplemental Table 2 Testing of linearity

Δ BIC > 4 indicates that the smoothing spline model yield a better account of the data than the linear model, while BIC $\leq$ 4 indicates that a linear fit to the data are the most appropriate.

Bold indicates ΔBIC $\geq$ 4

BIC: Bayesian Information Criterion